

Article

Not peer-reviewed version

Numerical Approach to Determine the Resistance of Threaded Anchors in UHPFRC

[Antonina Hochuli](#) ^{*} and [Eugen Brühwiler](#)

Posted Date: 27 September 2024

doi: 10.20944/preprints202409.2131.v1

Keywords: short anchorage; threaded anchor; numerical simulation; structural behavior; pull-out force



Preprints.org is a free multidiscipline platform providing preprint service that is dedicated to making early versions of research outputs permanently available and citable. Preprints posted at Preprints.org appear in Web of Science, Crossref, Google Scholar, Scilit, Europe PMC.

Copyright: This is an open access article distributed under the Creative Commons Attribution License which permits unrestricted use, distribution, and reproduction in any medium, provided the original work is properly cited.

Article

Numerical Approach to Determine the Resistance of Threaded Anchors in UHPFRC

Antonina Hochuli ^{1,*} and Eugen Brühwiler ²

¹ Transport and Mobility Laboratory, Institute of Structural Engineering, EPFL - Swiss Federal Institute of Technology, Swiss Federal Institute of Technology (EPFL)

² Institute of Structural Engineering, Swiss Federal Institute of Technology (EPFL)

* Correspondence: antonina.hochuli@epfl.ch

Abstract: Due to its relatively high tensile strength and dense matrix, UHPFRC has proven to be a highly effective building material for both strengthening existing reinforced concrete structures and constructing new ones. In both cases, the use of fasteners is prevailing, with threaded anchors being frequently employed. The thicknesses of structural components made of UHPFRC are relatively thin, i.e., at least 30mm, typically 50 to 100mm, and exceptionally 100 to 200mm. Therefore, the aim is to use fasteners with short anchorage lengths. In this study, the structural behavior of a short threaded anchor with a 20 mm diameter and an embedment length of 50 mm (2.5Ø) in UHPFRC is investigated using non-linear Finite Element models. UHPFRC is assumed to exhibit tensile strain-hardening behavior, with tensile strengths of 7 MPa and 11 MPa, respectively. The modelled anchor was subjected to a continuously increasing uniaxial pull-out force. The results indicate that the fracture mechanism of threaded anchors in UHPFRC is primarily characterized by the formation of a tensile membrane within the UHPFRC, which acts as the main resisting element against the pull-out force. Additionally, the influence of UHPFRC's tensile properties on the pull-out behavior and ultimate resistance of the threaded anchors was determined.

Keywords: short anchorage; threaded anchor; numerical simulation; structural behavior; pull-out force

1. Introduction

1.1. Industrial Demands and Research Motivation

The use of Ultra-High Performance Fibre Reinforced Cementitious Composites (UHPFRC) in structural engineering, particularly for constructing thin structural elements such of façades, bridges, and highly stressed fixed railway tracks, has revealed a need for anchorage systems with short embedment lengths. Current commercial anchorage systems were originally designed for concrete applications, with a minimum length of 80 mm, which is non-applicable for the constructive design of UHPFRC structural elements with thicknesses between 30 mm and 100 mm.

A recent application in the domain of fixed railway tracks [1] involved replacing damaged concrete monoblocs of 24 cm height by 11.9 cm-thin UHPFRC pedestals after only 40 years of operation. A comparison of project variants showed that, due to its relatively high mechanical strength and durability, UHPFRC can provide significantly more effective engineering solutions, both economically and technically, compared to traditional reinforced concrete. One of the challenges in this project was to define rail fasteners that were compatible with the entire fastening system. These fasteners had to be 20 mm in diameter but required a short embedment length. Additionally, the pull-out resistance of the anchorage in UHPFRC had to be determined. This project highlighted the need to further investigate the pull-out resistance of short anchors to optimize UHPFRC-based fixed railway track systems.

Moreover, the mentioned minimal anchor embedment length of 80 mm in concrete presupposes anchoring within the reinforcement layer near the surface. The pull-out resistance of such anchors in

concrete has been well-studied through numerous laboratory tests and investigations, resulting in four main fracture modes [3]: (a) Pull-out of a concrete cone, (b) Fracture of the anchor, (c) Pull-out of the anchor, and (d) Combined fracture of the concrete cone and anchor pull-out.

Since UHPFRC has significantly different properties from concrete, particularly in terms of tensile strength, fatigue resistance, and ductile deformation behavior, the fracture modes shown in Figure 1 for concrete cannot be directly adopted for UHPFRC.

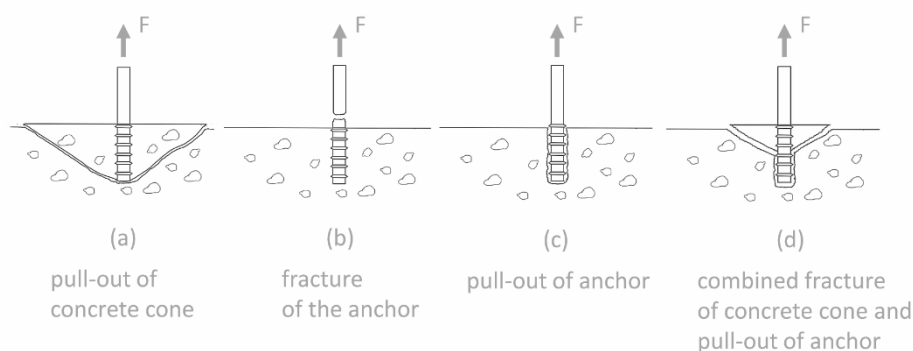


Figure 1. Schematic presentation of the fracture modes of cast-in-place threaded steel anchors in concrete or cementitious material with low tensile strength according to [7].

1.2. Research Objective

The main objective of this research is to investigate the structural behavior of UHPFRC under quasi-static, continuously increasing forces applied to short threaded anchors. This will be achieved by using non-linear finite element analysis as the first step in the investigation process.

To the best of the author's knowledge, no study is currently available on the structural behavior and pull-out resistance of UHPFRC, with tensile properties as shown in Figure 1, for anchors with short embedment lengths subjected to pull-out loading.

2. Materials and Methods

2.1. UHPFRC Material Properties

The Ultra-High Performance Fibre Reinforced Cementitious Composites (UHPFRC) is composed of a cementitious matrix of optimized high packing density, which is strengthened by a high amount of short, slender steel fibers. It has a compressive strength of more than 150 MPa and a tensile strength of more than 12 MPa while developing pronounced tensile strain-hardening and strain-softening behavior [6]. A further relevant property of UHPFRC is its extremely low permeability for water, leading to a highly durable material.

The UHPFRC response in tension (Figure 2) and compression is fundamentally different. Under direct compression, the material remains quasi-elastic almost until reaching the compressive strength. Under direct tension, three domains of material behavior are observed: (1) the elastic domain until the elastic limit stress f_{Ute} is reached, (2) beyond, quasi-linear strain hardening occurs when matrix discontinuities form, until the tensile strength f_{Utu} is attained, and (3) gradual softening of a single discrete crack in the weakest cross-section of the specimen, finally leading to material fracture. The fracture zone (3) is a transitional regime of a so-called fictitious crack, developing from a continuum to a real (stress-free) crack.

In addition, the fatigue endurance limit has been determined to be at a maximum fatigue stress level of 70% of the elastic limit stress for UHPFRC subjected in the elastic domain, at about 55 – 65% of the elastic limit stress for UHPFRC subjected in the strain hardening domain and 45% in the strain softening domain.

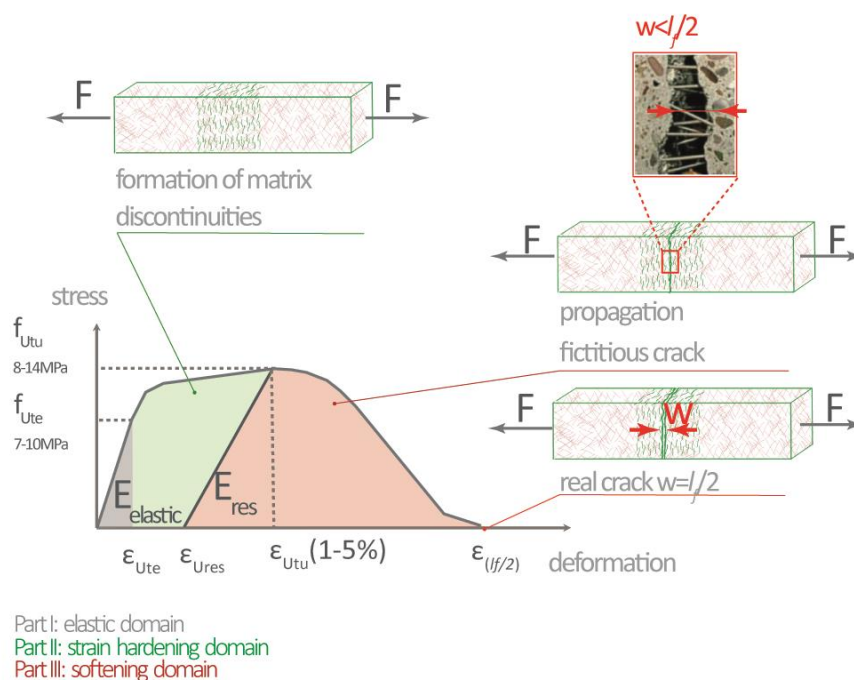


Figure 2. Tensile response of UHPFRC.

2.2. Methodology

To determine the failure mechanism of short threaded anchors embedded in UHPFRC and their pull-out resistance, a numerical approach was found to be efficient. The tensile and compressive properties of UHPFRC had already been tested through many uniaxial tensile and bending tests [2], [5]. These tests were used to calibrate the simulated material properties for the numerical model, which was subjected to a continuously increasing uniaxial pull-out force.

The numerical analysis was conducted using the finite element software ATENA[12]. The suitability of this program for the intended purpose was confirmed by the first author's prior experience in investigating damage of load-bearing structures made of reinforced concrete, including the Gotschna road tunnel and the Adler railway tunnel in Switzerland. Additionally, ATENA was used for designing rehabilitation measures for the fixed railway track at Zurich Airport station using UHPFRC [1,2]. In the damage investigations of the mentioned tunnels, monitoring was conducted, which validated the results of the numerical analysis.

In the frame of this research, the numerical modeling was carried out as follows:

1. Simulation of previously conducted 4-point bending tests, following [4] (pp. 4-5), using UHPFRC properties from test B4 (p.6). The numerical model was also tested using UHPFRC properties of specimen T1-2 from [3] (p.5 Table 2, p.9) and specimen TIII 000-1 from [5] (p.19 Table 3.2, p.94). The simulated 4-point bending test served as an auxiliary model.
2. Calibration of the finite element mesh using the auxiliary model.
3. Simulation of the numerical model to investigate pull-out resistance.
4. Sensitivity analysis and calibration of the finite element mesh size.

The geometry of the steel anchor was slightly modified for numerical purposes; the flanks of the threaded anchor were modeled with the same surface, thread angle, and pitch as a B500B rebar with a diameter of 20 mm, but without a helix angle.

2. Literature Review

Previous laboratory tests were mainly conducted on fiber-reinforced concretes, high performance fiber-reinforced concretes, or different types of UHPFRC with low steel fiber content, usually 0.1 % – 1.6 %. In addition, epoxy glue and other synthetic materials were used as bonding materials for anchors. In some cases, UHPFRC itself was used as a bonding material for post-installed

anchors in concrete [4]. All reported laboratory tests failed by anchor pull-out (Figure 1(c)), fracture of the anchor (Figure 1 (b)), or a combined fracture (Figure 1 (d)), except the particular type of facade anchors discussed below. Thus, the pull-out resistance of UHPFRC could not be directly determined, nor could the structural behavior be investigated based on these laboratory tests.

Satoh et al. [4] conducted pull-out tests on post-installed adhesive anchors in concrete, which were fixed in a borehole of 30 mm diameter using UHPFRC and analyzed the results using a finite element model. The anchors with 25 mm, 50 mm, and 75 mm embedment lengths were tested. The UHPFRC, with a compressive strength of 100 MPa and tensile strength of 10 MPa, had a fiber content of only 1.57 vol. %. The tests revealed that the pull-out of a concrete cone (similar to Figure 1 (a)) occurs in the case of the shortest anchor with an embedment length of 25 mm, and the combined fracture mode was observed in the case of 50 mm and 75 mm embedment lengths (Figure 1 (d)). This research showed that using UHPFRC instead of the grouting mortar increases the bond between anchor and concrete and thus increases the pull-out resistance of anchors fixed in concrete. In addition, the finite element analysis [4] showed that critical cracks appeared in concrete and led to the formation of the fracture cone.

Kalthoff et al. [5] investigated the pull-out behavior of threaded anchors with a relatively short pitch in UHPC (ultra-high performance concrete) with 0.62% to 1.86% fiber content and concrete. The pull-out resistance in the tested UHPC was up to 53% higher than in concrete. Moreover, it was pointed out that using short anchors in concrete is unreliable and thus not recommended. A good bond was achieved just in the case of anchorage in UHPC. Furthermore, the same fracture mechanism for UHPC and concrete was initially assumed. However, no specific investigation of fracture mode was conducted, and thus, the results could not be used for the interpretation of the fracture mechanisms observed in this work.

Fehling and Lorenz [6] investigated the bond behavior of rebars in UHPC. They performed three series of pull-out tests on rebars with diameters $d_s = 12$ mm and 14 mm anchored in UHPC with 0.1% to 1.5% steel fiber contents, in which different parameters were varied:

1. The first test series investigated the influence of UHPC cover thickness on the fracture mode. The pull-out force was applied to the rebars with embedment lengths ranging from $2d_s$ to $12d_s$ anchored in the UHPC specimens with the UHPC cover of d_s to $2.5d_s$. It was found that the increase of UHPC cover leads to the disproportionately lower increase of the average bond strength at maximum force. Furthermore, splitting of UHPC was observed in the case of rebars with an embedment length of $8d_s$ anchored in UHPC of 1% fiber content and UHPC-cover smaller than $2.5 d_s$.
2. The effect of conventional steel reinforcement bars deployed in the transverse direction was investigated in the second series. The pull-out force was applied to the rebars with an embedment length of $2d_s$ to $5d_s$ anchored in the specimens with a UHPC cover of $1d_s$ to $2.5d_s$. The results show that transverse reinforcement bars do not increase the pull-out resistance in the tested case.
3. The influence of fiber content on bond strength was investigated in the third series, which was performed on the UHPC specimens of the length of 780 mm, width of 300mm, and height of 360 mm with the anchored rebars with embedment lengths of $3.5d_s$ and $5d_s$. The steel fiber content was 0.5, 1 and 1.5%. The type of fibers and the heat treatment were the same as in the second test series. The UHPC cone fracture type was observed in the case of UHPC cover larger than $2d_s$ and embedment length of $3.5d_s$ to $5d_s$. In the case of a very large (not exactly defined) UHPC cover, a combination of UHPC-cone and splitting cracking was observed.

The tests reveal that UHPC with fiber content up to 1.5% behaves similarly to concrete. Thereby, the UHPC cone fracture in analogy to Figure 1 (a) occurs just in the case of the shortest embedment length, which was of sufficient size to allow for fracture cone formation. Moreover, on the photo showing the fracture mode (Figure 7 in [6]), radial cracks are identified, which indicates that the tensile strength of UHPC in the tangential direction around the rebars was reached.

Grzesiak et al. [7] investigated facade anchors fixed in high-performance polypropylene fibre reinforced concrete (HPFRC). The stiff polypropylene fibres with a diameter of 0.70 mm and a length of 30 mm are three times larger than usual steel microfibers (for instance, the steel microfibers in a

commercially available UHPFRC-mix are 13 mm long and have a diameter of 0.175 mm). Two types of facade anchors with an embedment length of 25 and 26 mm were used. In both cases, the fracture mode was a pulled-out HPFRC cone, which is very similar to the typical fracture cone in concrete, according to Figure 1 (a). Thereby, the inclination between the fracture surface and the specimen surface was about 35°. In the case of the adjustable suspended tension anchor, the pull-out resistance of the HPFRC cone increased up to 250% with increasing polypropylene fibre content from 10 to 35 kg/m³. The pull-out tests for the adjustable spacer bolt showed no significant improvement in the pull-out resistance due to increased fiber content.

The research findings indicate that increasing steel microfibre content increases the pull-out resistance. Generally, a better bond can be achieved between a threaded steel anchor and UHPFRC than in concrete. With increasing steel microfibre content, the fracture mechanism changes from a pure fracture cone, according to Figure 1 (a), to a combined fracture mechanism, according to Figure 1 (d). Furthermore, in UHPFRC with polypropylene fibers, just as in a steel fiber-reinforced concrete, an increase in the pull-out resistance of the fracture cone is observed. The fibers that traverse the fracture surface are anchored on both faces of the crack, transmitting tensile stress.

3. Numerical Simulation

3.1. Aim

Current non-linear FE programs allow for accurate modeling of the properties of cementitious building materials and structural elements to simulate the structural behavior up to maximum resistance and into the post-peak domain. These FE models are often used for detailed analysis of laboratory test results and investigation of the mechanical behavior of structures, considering specific loading conditions. Such finite element simulations presuppose that the cementitious building material is idealized as a continuum with a predefined constitutive stress-strain law.

In the following, the structural behavior of UHPFRC near a short, threaded anchor subjected to uniaxial quasi-static loading is investigated by means of non-linear finite element analyses. Moreover, it will be demonstrated that numerical simulation is an efficient approach for designing laboratory tests or in-situ monitoring of structures.

3.2. Numerical Model

The presented numerical model corresponds to a common and frequently encountered application scenario for increasing the load-bearing capacity of a reinforced concrete (RC) slab due to the application of a UHPFRC layer and the need to fix a tensile element on the top of a slab. To the existing RC element, a 50 mm thin layer of UHPFRC is added. An alternative application case to the building of the numerical model could also be a model that represents a thin UHPFRC structural part, but, in this case, an additional boundary condition would be needed to obtain compliance of this thin structural part under the pull-out force.

Further, as known from numerous laboratory tests and realized projects, a monolithic bond is obtained between the concrete and the UHPFRC layer. Thus, the numerical model assumes a monolithic bond between both building materials and that no cracking or fracture occurs in the concrete layer below the anchor. Based on this, assigning only UHPFRC properties to the macro-elements representing the UHPFRC part of the composite slab is sufficient, making the numerical analysis easier and more efficient. Figure 3(a) presents the concept of the numerical model. A rectangular element ① of 0.5m×0.5m×0.5m is cut out from a large composite slab, consisting of a concrete part with a thickness of 0.45 m and a UHPFRC layer of 50 mm, which are monolithically connected. A short, threaded anchor of 20 mm diameter ②, with an embedment length of 50 mm and six force-transmitting flanks, is fixed in the UHPFRC layer during casting. The size of the anchor flank surface corresponds to a common rebar. Figure 3 (b) shows the numerical model using the finite element program ATENA [8]. The anchor is modeled with six 5 mm wide flanks distributed evenly along the embedded part according to Figure 4. Because of the non-orthogonal shape, the tetrahedra mesh with an element size of 3 mm was assigned to the anchor. The simulated slab part is subdivided

into three areas. The inner orthogonal macro element around the anchor with a size of $0.1\text{m} \times 0.1\text{m} \times 0.1\text{m}$ (Figure 3 (b)) has the same mesh type and size as the anchor. The macro-element anchor and the macro-element UHPFRC are monolithically connected to simulate the UHPFRC – steel bond behavior. The outer upper area of the UHPFRC element is subdivided into eight orthogonal macro elements, to which the hexahedra mesh type of the element size of 23 mm was assigned. The lower area of the UHPFRC element serves only for self-weight and is statically irrelevant, as only the upper area will be affected, as shown below. This area was subdivided into nine orthogonal macro elements with hexahedra mesh of 100 mm element size for geometrical reasons. All macro elements representing UHPFRC are monolithically connected. The size of finite elements in the numerical model was iteratively determined, calibrated using the auxiliary model according to 2.2 and tested to ensure force transmission from the anchor to the UHPFRC over the surfaces of the flanks.

Note that the size of the representative slab part (Figure 3 (a)) has been chosen so that the horizontal supports ④ are placed outside the area with UHPFRC – anchor interaction. The self-weight of this representative slab part is greater than the maximum pull-out force, such that the reaction of the vertical support ③ is always in compression. In addition, since the focus is to analyze the structural behavior of UHPFRC and how the pull-out force is introduced in UHPFRC structural parts, the numerical simulation of anchor slip in UHPFRC is not performed, since the term slip refers to the limited abrupt displacement of the anchor, during which no force is introduced into the UHPFRC. A sensitivity analysis was performed to justify this assumption. For this, the interface elements between the anchor and the UHPFRC macro-elements were inserted into the original model, and the horizontal stiffness (friction) was varied. This sensitivity analysis showed that no slip was observed even at very low friction in the case of this specific numerical model, and as a result, the compressive force introduced in UHPFRC above the anchor flanks remains the same during each loading step in the numerical models with and without interfaces. The only difference between both models obviously was the computing time, which was longer in the case of the model with interfaces. This sensitivity analysis does, however, not claim that a slip between UHPFRC and the anchor could not occur in real structural elements.

Further, Figure 4 shows the concept of force introduction from the threaded anchor into the UHPFRC bulk material, as considered in the numerical model. The applied pull-out force causes tensile stress in the anchor, which leads to compressive stress acting on the contact surfaces between the anchor flanks and the UHPFRC. The resulting inclined upward compressive stress fields in UHPFRC lead to the formation of a horizontal near surface tensile stress field in UHPFRC, as will be discussed below. The maximum compressive force that can be introduced into the UHPFRC over a flank is limited by the compressive strength of UHPFRC.

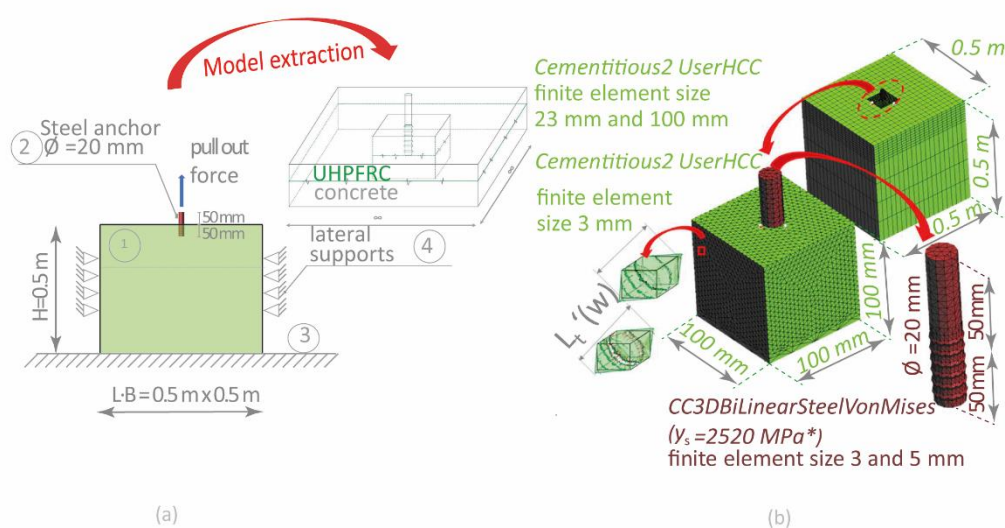


Figure 3. (a) Schematic illustration of the set-up; (b) numerical model and illustration of the formation of discontinuities and propagation of a fictitious crack in finite element.

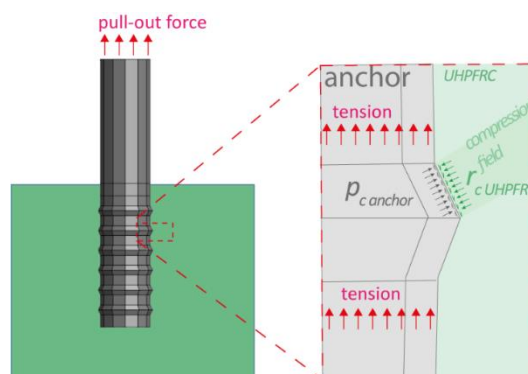


Figure 4. Stress transfer from steel anchor to UHPFRC along the contact surface of the anchor rib with the UHPFRC.

3.3. Modeling of UHPFRC

The theoretical background of the numerical modeling of UHPFRC and the programming aspects are described in detail in [13]. The following is the summary of the relevant steps of numerical computation in ATENA. Table 1 summarizes the mechanical properties of two UHPFRC products used in this study. Both commercially available UHPFRC products were already used in previous research for laboratory tests. UHPFRC 7 corresponds to TIII 000-1 according to [5] (p. 94) and UHPFRC 11 corresponds to T1-2 according to [3] (p.9).

The mechanical properties of UHPFRC were modeled using a fracture-plastic material model (CC3DNonLinCementitious2User [13]), in which the constitutive models for tensile and compressive behavior are combined. The fracture model is based on the smeared crack model that presupposes the Rankine failure criterion. A pointwise defined tensile softening law close to a linear function is used (Figure 5). The plasticity model is based on the Menétrey-Willam failure surface. The fracture and plasticity models are combined by the strain decomposition method after De Borst [14] [13] and the return mapping algorithm is used to determine the elastic predictor. Due to strain decomposition after De Borst [14] into elastic ε_{ij}^e , plastic ε_{ij}^p , and fracture ε_{ij}^f components ($\varepsilon_{ij} = \varepsilon_{ij}^e + \varepsilon_{ij}^p + \varepsilon_{ij}^f$, $i, j = 1, 2, 3, 4$), the stress equivalence in both models is guaranteed. The new stress state is determined according to the formula $\sigma_{ijn} = \sigma_{ijn-1} + E_{ijkl}(\Delta \varepsilon_{kl} - \Delta \varepsilon_{kl}^p - \Delta \varepsilon_{kl}^f)$, where the $\Delta \varepsilon_{kl}^p$ and $\Delta \varepsilon_{kl}^f$ are increments of plastic and fracture strain. As mentioned above, the Rankine criterion $F_{ij} = \sigma_{ijt} - f_{ti} \leq 0$ is considered in the numerical simulation of the softening behavior [13], where σ_{ijt} is the tensile stress calculated according to the formula: $\sigma_{ijt} = \sigma_{ijn-1} + E_{ijkl}(\Delta \varepsilon_{kl}^{calc} + \Delta \varepsilon_{kl}^p + \Delta \varepsilon_{kl}^f)$, f_{ti} is the tensile strength in the principal stress direction i , and k is the failure surface. If the calculated tensile stress σ_{ijt} is higher than the tensile strength f_{ti} , then, in the next iteration step n , the tensile stress is recalculated such that the final tensile stress satisfies the condition: $F_{ij} = \sigma_{ijn} - f_{ti} = 0$.

Assuming that the increment of fracture strain $\Delta \varepsilon_{kl}^f$ is normal to the failure surface k , it follows that $\Delta \varepsilon_{kl}^f = \Delta \lambda \cdot \partial F_{kf} / \partial \sigma_{ij} = \Delta \lambda \cdot \delta_{ik}$, where $\Delta \lambda$ is the increment of the fracturing multiplier. By the substitution of the tensile stress $\sigma_{ijn} = \sigma_{ijt} - E_{ijkl} \cdot \Delta \varepsilon_{kl}^f$ and the increment of the fracture strain $\Delta \varepsilon_{kl}^f$ into $F_{ij} = \sigma_{ijt} - f_{ti} = 0$, the fracturing multiplier is determined as follows: $\Delta \lambda = (\sigma_{kkt} - f_{tk}) / E_{kkkk}$. Further, the crack opening $w_{k \max}$ is determined by the sum of the total value of the fracture strain ε_{kkf} and the current increment of the fracturing strain $\Delta \varepsilon_{kkf} = \Delta \lambda \cdot \delta_{kk}$, multiplied by the characteristic length L_t : $w_{k \max} = L_t(\varepsilon_{kkf} + \Delta \varepsilon_{kkf})$. It should be noted that, in the present study, the characteristic length L_t is defined as the projection of

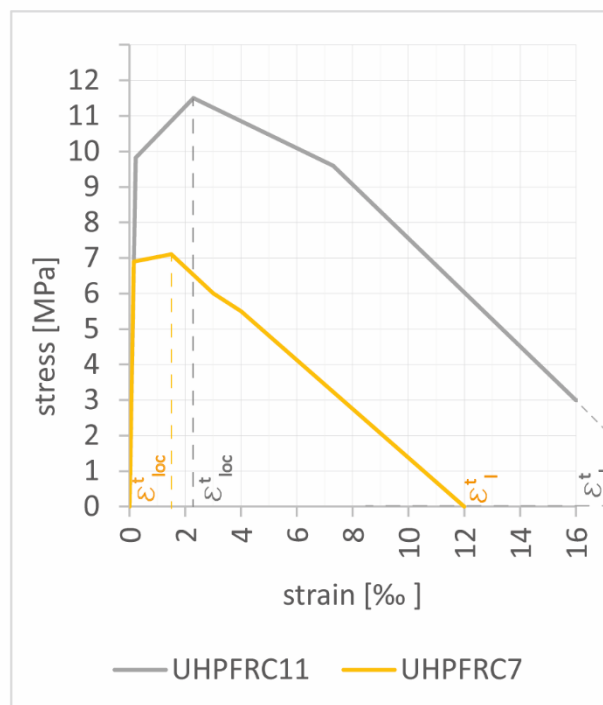
the geometric size of the finite element on the axis in the direction of the principal strain and corresponds to the characteristic crack¹ bandwidth [11], as shown in Figure 3 (b).

Further, Figure 5 presents the tensile law of UHPFRC, modeled pointwise in the elastic, strain-hardening, and strain-softening domains. Until the localization of strain (ϵ_{tloc}), the stress-strain curve corresponds to the stress-strain constitutive law. After exceeding the localized strain ϵ_{tloc} , the material law is adjusted to the actual crack band L_t [16] as follows: $\epsilon_{fl\ current} = \epsilon_{tloc} + (\epsilon_{fl} - \epsilon_{tloc})/L_t/L_{tch}$, thereby, L_{tch} is the measuring base used to determine the strain value.

Note that the mentioned crack band model was initially developed for concrete. Since concrete is a cementitious material with low tensile strength and without strain-hardening domain, tensile strain softening occurs immediately after reaching the tensile strength when the fictitious crack starts to develop. Unlike concrete, UHPFRC shows matrix discontinuities and no real crack until reaching the deformation w ($\epsilon_{fl} = l_f/2$) corresponding to half of the maximum fiber length l_f . Therefore, the crack band model can be interpreted as a discontinuity band model in the case of UHPFRC.

Table 1. Tensile properties of the two used UHPFRC products.

Tensile properties of UHPFRC according to [3] (p.5 Table 2, p.9) and [5] (p.19 Table 3.2, p.94)		UHPFRC11	UHPFRC7
Tensile strength	f_{Utu} [MPa]	11.5	7.1
Elastic limit	f_{Ute} [MPa]	9.8	6.9
Strain in UHPFRC at the tensile strength	ϵ_{Utu} [‰]	2.29	1.5
Strain in UHPFRC at the elastic tensile strength	ϵ_{Ute} [‰]	0.22	0.15
Fiber length	l_f [mm]	13	13
Fiber diameter	d_f [mm]	0.175	0.16
fiber content	Vol. [%]	3.8	3.0



¹ The definition of "crack" in the case of UHPFRC means multiple fine cracking of the cementitious matrix of UHPFRC. Tensile stress is transmitted by the steel fibres. In this paper, this type of cracking is called "matrix discontinuity".

Figure 5. Assumed tensile stress-strain curves based on the tensile properties of the two UHPFRC products according to Table 1.

4. Numerical Simulation of the Quasi-Static Structural Behavior of UHPFRC Substrate

4.1. Modeling of Quasi-Static Loading

The quasi-static pull-out force is modeled as a gradually increasing uniaxial force with 5kN per loading step acting at the top of the steel anchor. To simulate the post-peak domain, the arc-length solution method was used [13]. Note that for studying this model, knowing the exact force introduced into the UHPFRC body is crucial. Therefore, the introduced force in the UHPFRC body is monitored on the level of the top UHPFRC surface, as shown in Figure 7. This modeling results in pull-out force–displacement curves shown in Figure 6. The finite element simulation ran until no more change of the introduced pull-out force was observed in the post-peak domain. The numerical simulation was interrupted manually when at constant pull-out force the displacement at point O (Figure 7) was increasing which was interpreted as pulling out of the threaded steel bar from the UHPFRC substrate.

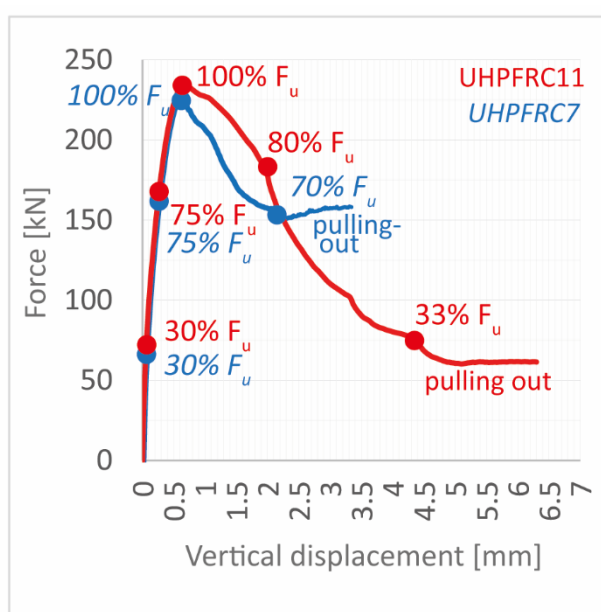


Figure 6. Force-Displacement Diagram UHPFRC7 and UHPFRC11.

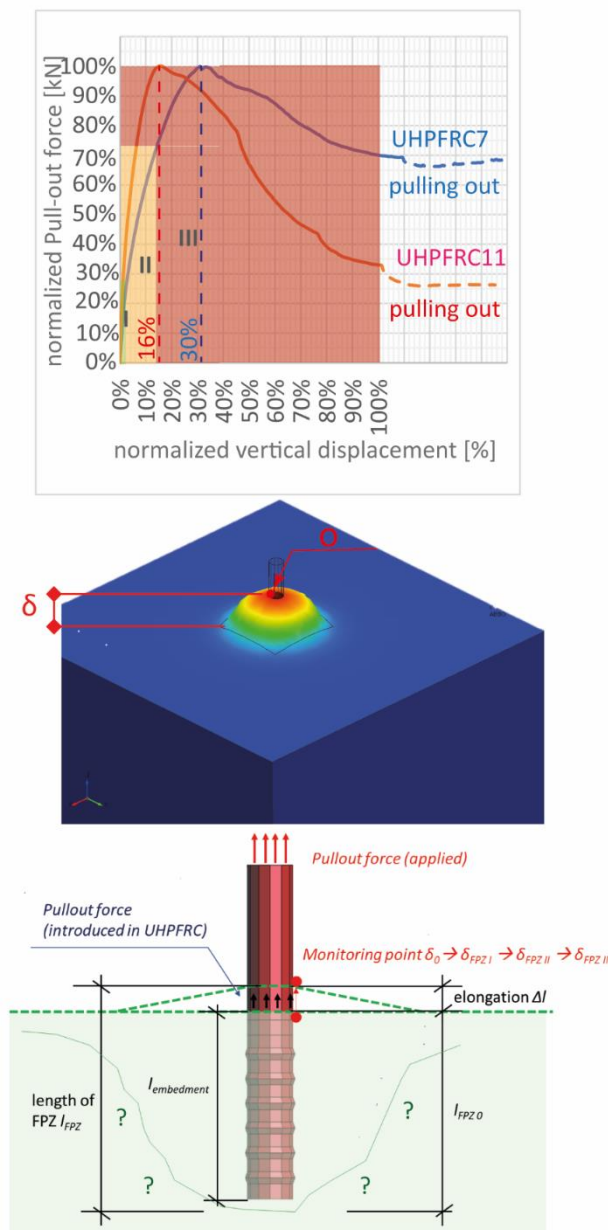


Figure 7. Normalized pull-out force–displacement diagrams for pulling the threaded anchor $\varnothing 20$ mm $l_{embedment} = 50$ mm out of two different UHPFRC types.

5. Results

5.1. Pull-Out Force-Displacement Curves

To investigate the effect of increasing the tensile strength of UHPFRC on the force–displacement behavior and the fracture mode, the force–displacement diagram was normalized. Figure 7 presents the normalized pull-out force–displacement curves obtained for UHPFRC11 and UHPFRC7. Thereby, the maximum vertical displacement is assumed to be the displacement at which no more force change was registered; respectively, the threaded anchor will be pulled out from the UHPFRC substrate. It can be seen that the ultimate force F_u of the anchorage was achieved at 16% of the maximum vertical displacement for UHPFRC11 and 30% of the maximum displacement for UHPFRC7.

Analysis of the absolute magnitudes of force and displacement (Figure 6) reveals that the computed ultimate force of the anchorage is similar, i.e. 234 kN in UHPFRC11 and 227 kN in

UHPFRC7, reached at the same vertical displacement of 0.7 mm in both cases. However, the post-peak domain is different. In UHPFRC7, the post-peak domain shows relatively little deformation while the force decreases to 70% F_u with increasing vertical deformation thereafter at constant force, indicating pulling-out mechanism. In the post-peak domain of UHPFRC11, the force decreases to 33% F_u , then only the vertical deformation near the anchor increases.

In both cases, no real crack occurs in the tensile membrane during the entire loading process. The strain increase in the membrane leads to a widening of the opening between UHPFRC and the anchor. This means that the ultimate force of the anchorage does not correspond to the ultimate resistance of the UHPFRC membrane. Moreover, the numerically simulated pull-out behavior shows three domains with different slopes, corresponding to three stages of the pull-out process. Therefore, for the detailed analysis of the numerical results, the entire loading process is subdivided into three phases: Phase I: loading up to 30% F_u , Phase II: loading up to 75% F_u , and Phase III: loading up to 100% F_u and post-peak. Using plots of principal strains at each loading phase and in the post-peak domain, the tension and compression fields and, thus, the fracture process are analyzed as follows.

5.2. Pull-Out and Fracture Process

Figures 9 (a) and (b) show plots of maximum principal strain at the end of phases I, II, and when achieving 100% F_u . These plots are supplemented with red and blue arrows to clarify the development of tension and compression fields. The red arrows highlight the tensile strain propagation in the radial direction, and the blue arrows show the direction of the compression field extension extracted from the plots of minimum principal strain. Positive values of principal strains correspond to tension and negative values to compression.

In phase I, which extends from 0 kN to 30% F_u , the pull-out process starts to propagate in the upper part of the UHPFRC layer around the threaded anchor within an approximately 5 mm thin horizontal circular tension strain field (ϵ_{rad}). Additionally, an inclined tensile strain field (ϵ_{cone}) develops perpendicular to the UHPFRC cone forms.

These strain fields reveal that the pull-out force introduced via the threaded anchor produces initially conical compression ($-\epsilon$) and circular horizontal tension fields (ϵ_{rad}) in the near surface UHPFRC layer. If no fracture of the steel anchor occurs, and compression ($\sigma_{compression}(-\epsilon) \leq f_{uc}$) and tension ($\sigma_{tension}(\epsilon_{rad}) \leq f_{tu}$) are transmitted in the UHPFRC substrate, the anchorage is functional. Thereby, the UHPFRC next to the threaded anchor enters into the strain-softening domain, already at $F=10-15\%$ F_u . UHPFRC in the softening domain in the state at the end of phase I (30% F_u) is shown with the orange color for UHPFRC7 and the purple color for UHPFRC11 according to the scale on the right of Figures 9 (a) and (b). Further, the inclined tensile strain field (ϵ_{cone}) extends over the entire UHPFRC region that comprises the threaded anchor and the UHPFRC cone, including the mentioned circular horizontal tensile (ϵ_{rad}) and conical compression ($-\epsilon$) strain fields. In addition, phase I is characterized by the quasi-linear path on the force-displacement diagram indicating elastic behavior.

During phase II, extending up to 75% F_u , the horizontal circular tensile strain field (ϵ_{rad}) increases further and encompasses the UHPFRC cone (l_{cone}) completely, as depicted by the plots of principal strains.

Moreover, with increasing circular tension strain field (ϵ_{rad} , $l_{membrane}$), the height of the UHPFRC cone decreases ($l_{cone} \rightarrow 0$). And at the end of phase II, the anchorage mechanism consists of alone the circular tension field of thickness ($l_{membrane}$) which is equal to the embedment length of the threaded anchor $l_{embedment}$. From a static viewpoint, the circular tension strain field (ϵ_{rad}) behaves like a tensile membrane. On the force-displacement diagram, phase II is characterized by non-linear force-displacement behavior between 30% F_u and 75% F_u .

Phase III begins with the fully formed tensile membrane of thickness $l_{membrane} \approx 1.0-1.1 l_{embedment}$ as the main resisting part against the pull-out force. Since the pull-out force acting through the threaded anchor leads to compression at the contact surfaces between the anchor flanks and UHPFRC (Figure 4), the inclined conical compression strain field ($-\epsilon$, Figure 8 (a) and (b)) is also observed within the tensile membrane and causes additional increasing tensile strain in the upper third of the tensile membrane.

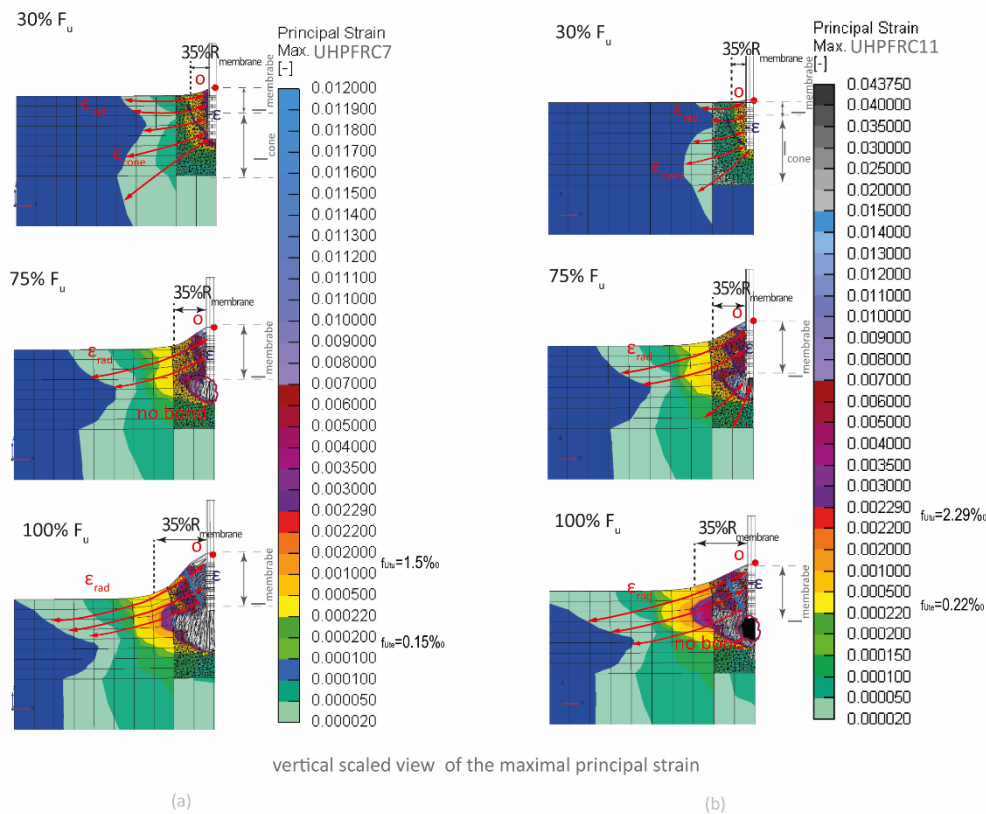


Figure 8. (a) Development of the membrane in the UHPFRC7 (Output ATENA principal strain max) **(b)** Development of the membrane in the UHPFRC11 (Output ATENA principal strain max).

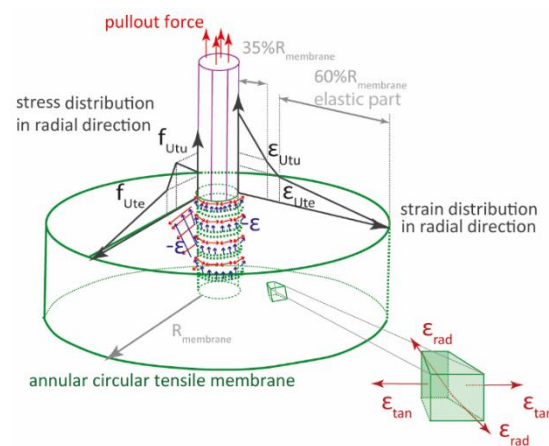


Figure 9. Schematic representation of the stress and strain distribution within the tensile membrane.

5.3. Failure Process within the Tensile Membrane

Next, the failure process within the tensile membrane is analyzed. Figure 9 presents schematically the strain (ϵ_{rad}) and stress (f_i) distribution within the tensile membrane. Figures 12 and 13 show the state of the strain distribution in the radial direction (ϵ_{rad}) in the annular circular tensile membrane every 54 kN until F_u is reached. The step of 54kN was chosen iteratively to monitor the development of the tensile membrane. The dashed arrows indicate the radius of the tensile membrane that corresponds to the loading given on the dashed arrows. According to the legend below the diagrams, the color curves present the strain distribution within the tensile membrane in the mentioned loading steps. From these diagrams, the development of the tensile membrane and the

strain distribution during the entire loading process can be depicted. The diagram shows that the maximum radius ($R_{membrane}$) is 250 mm, and the outer part of the membrane, corresponding to 60% of the membrane radius, remains in the elastic domain during the entire loading process. UHPFRC next to the anchor enters into the softening domain, still within the loading phase I according to Figure 7. The comparison of Figure 10 and Figure 11 reveals that the tensile membrane in UHPFRC11 is bell-shaped and more pronounced in the inner part than in UHPFRC7, whereas the tensile membrane in UHPFRC7 is less pronounced and shows the shape of an arch.

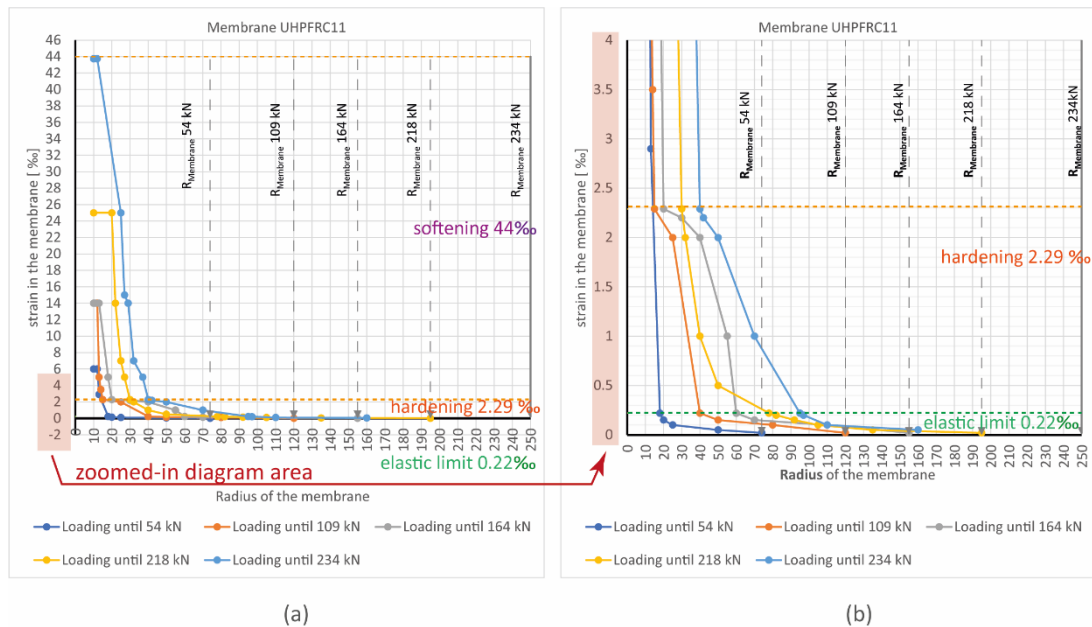


Figure 10. Strain-distribution in the tensile membrane for UHPFRC11: (a) strain distribution 0-44‰, (b) strain distribution 0-4‰.

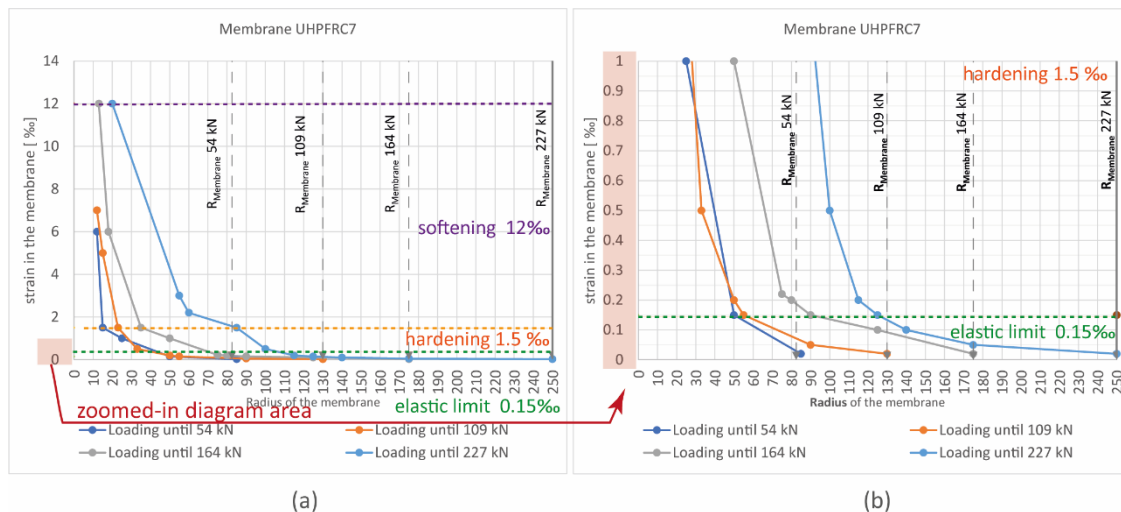


Figure 11. Strain-distribution in the tensile membrane for UHPFRC7: (a) strain distribution 0-14‰, (b) strain distribution 0-1‰.

Further, the diagrams shown in Figure 12 provide the main parameters, i.e., the radius of the tensile membrane $R_{membrane}$ and the thickness of the membrane $l_{membrane}$ during the loading process. During loading phases I and II, the tensile membrane forms, and the rate of increase in the radial direction is up to 5 times higher than in the vertical direction.

The tensile stress remains constant within a limited part of the membrane with a constant diameter where failure occurs. However, more volume is activated within the substrate around the

anchor where the tensile membrane develops, and the tensile stress is distributed such that the outer part of the tensile membrane, corresponding to 60% of the radius, remains elastic. Thus, the membrane maintains force balance during the entire loading process.

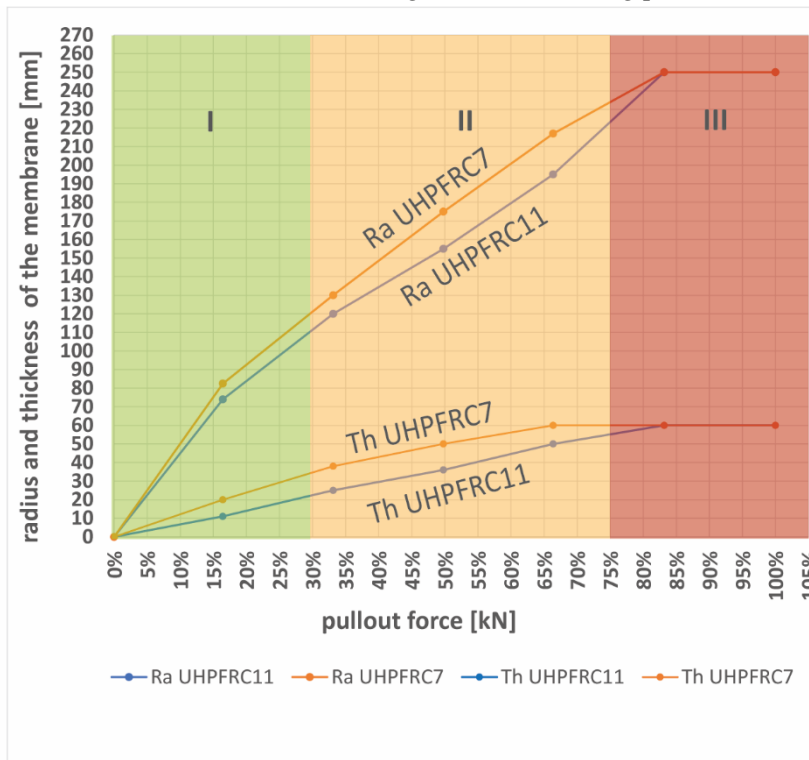


Figure 12. Radius (Ra) and thickness (Th) of the membrane, with increasing pull-out force.

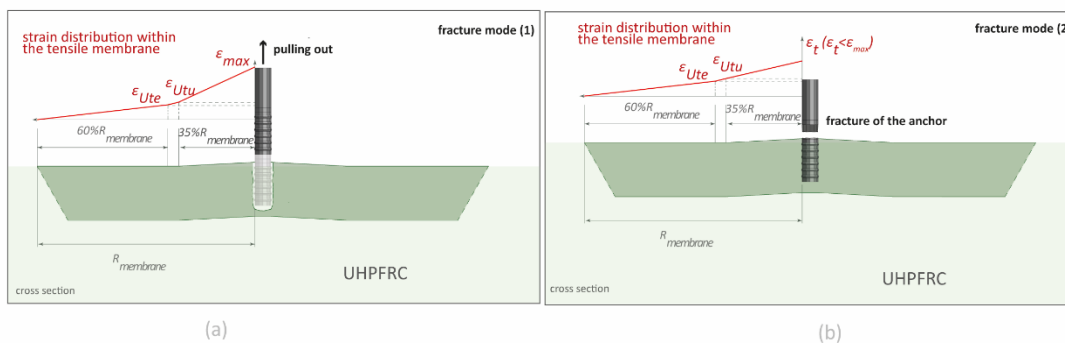


Figure 13. Failure modes of the threaded anchors in UHPFRC.

5.3. Features of the Failure Mode

This study aims principally to investigate the structural behavior of the anchorage of common threaded steel bars in UHPFRC with given tensile properties as subjected to pull-out force using finite element analysis. The investigation of the structural behavior of UHPFRC was possible because the numerical modeling allows to assign sufficiently high tensile strength to the steel to avoid anchor fracture such that the failure mechanism in UHPFRC becomes the determinant failure mechanism of the system.

The numerical simulations show that the introduction of a pull-out force in the UHPFRC body via a short, threaded anchor leads to the formation of a tensile membrane in the near surface UHPFRC with a thickness $1 - 1,1 \text{ lembedment}$. The outer part of this tensile membrane, which corresponds to about 60% of the membrane radius, remains in the elastic domain during the entire pull-out process while the thickness and radius of the tensile membrane increase. Thus, the fracture process zone is localized in the inner part of the annular circular tensile membrane of UHPFRC, corresponding to about 35%

of the membrane radius. In the radial direction, the tensile membrane develops up to 5 times faster than the thickness in the vertical direction. At about 85% of the ultimate force F_u , the tensile membrane is completely formed with the thickness corresponding to the anchor embedment length $l_{embedment}$ and radius of about $5 l_{embedment}$. The stress transfer in the completely formed tensile membrane occurs further via compressive stresses acting on the contact surface between anchor flanks and UHPFRC, forming compression stress fields and increasing tensile stresses in the upper third of the tensile membrane. Finally, anchorage failure occurs due to the widening of the inner part of the annular circular UHPFRC tensile membrane around the anchor and, as a result, pulling-out the anchor from the UHPFRC substrate. Thereby, no real cracks occur.

In summary, this study has revealed that the pull-out behavior of threaded anchors in a UHPFRC substrate fundamentally differs from the well-known pull-out behavior in concrete, according to Figure 1. For short, threaded anchors in UHPFRC, only two fracture modes are possible: (1) $F_{u,anchor} > F_{u,membrane}$: pulling-out of the threaded anchor from the UHPFRC substrate (fracture mode (1) Figure 13 (a)) , or (2) $F_{u,anchor} < F_{u,membrane}$: fracture of the anchor (fracture mode (2) Figure 13 (b)).

Another feature of the structural behavior of the anchorage system is the plastic deformation in terms of failure indication:

- In the case of the tensile resistance of the anchor being lower than the pull-out resistance of the UHPFRC substrate ($F_{u,anchor} < F_{u,membrane}$), the plastic deformation of the threaded anchor would occur. This is the relevant case for the design of anchors in structural applications in engineering practice.
- In the case of the tensile resistance of the anchor being higher than the pull-out resistance of the UHPFRC substrate ($F_{u,anchor} > F_{u,membrane}$), the tensile membrane deforms within the inner 35% of the tensile membrane radius $R_{membrane}$ around the anchor. Comparing the vertical deformations in UHPFRC11 and UHPFRC7 at the instant of anchorage failure, the vertical deformation of the annular circular tensile membrane with higher tensile properties was found to be more pronounced and localized around the threaded anchor. However, the vertical deformations remain very small compared to the fracture deformation of the anchor in steel. These vertical deformations are only 2mm for UHPFRC7 and 4.5mm for UHPFRC11. However, this failure mode can only occur if the threaded anchor of diameter 20 mm is made of high-strength steel ($f_t \geq 700\text{MPa}$).

The tensile stress remains constant within a limited part of the membrane with a constant diameter where failure occurs. However, more volume is activated within the substrate around the anchor where the tensile membrane develops, and the tensile stress is distributed such that the outer part of the tensile membrane, corresponding to 60% of the radius, remains elastic. Thus, the membrane maintains force balance during the entire loading process.

6. Conclusions

1. This study shows that FE modeling is an efficient approach to discover possible failure mechanisms before laboratory tests are designed to focus on the research-relevant case. FE modeling allows to vary building material properties such as to avoid failure modes that are not research-relevant, i.e., fracture of the steel anchor.
2. Due to the UHPFRC's relatively high tensile strength and tensile deformation capacity, significant tensile stress fields form a tensile membrane in the UHPFRC substrate near the anchor when subjected to increasing quasi-static pull-out force.
3. With sufficient substrate size (i.e., the distance from the anchor to the element edge should be longer than five times the embedment length of the anchor), the tensile membrane develops both in horizontal and vertical directions. The tensile membrane's maximum extension was about five times the membrane thickness in the horizontal radial direction.
4. The tensile membrane's outer part, corresponding to 60% $R_{membrane}$, remained in the elastic domain during the loading process until pulling-out of the threaded anchor.

- No fracture of the UHPFRC substrate was observed; the failure of the anchorage occurred due to the widening of the inner part of the UHPFRC annular circular tensile membrane and pulling out of the threaded anchor.

Author Contributions: Conceptualization, A.H. and E.B.; methodology, A.H, E.B.; validation, A.H., E.B; formal analysis, A.H.; investigation, A.H.; writing—original draft preparation, A.H.; writing—review and editing, E.B.; supervision, E.B.; All authors have read and agreed to the published version of the manuscript.

Funding: This research received no external funding.

Acknowledgments: This article is a revised and expanded version of the conference paper titled “Numerical Simulation of the Structural Behavior of Threaded Anchors in UHPFRC”, presented at the 3rd International Interactive Symposium on Ultra-High Performance Concrete, Wilmington, Delaware, USA, June 4-7, 2023 [17], and “Failure Mechanism of Threaded Anchors in UHPFRC as Simulated by Finite Element Analysis”, which will be presented at the 4th International Symposium on Ultra-High Performance Fibre-Reinforced Concrete (UHPFRC), Menton, France, October 21-23, 2024 [18].

Conflicts of Interest: The authors declare no conflicts of interest.

References

- Hochuli A, Brühwiler E, Trouillet J.-G., "Improvement of fixed railway tracks using fatigue-resistant cementitious fibre reinforced composite material, Proceedings of The Fifth International Conference on Railway Technology: Research, Development and Maintenance, ", Montpellier, France, <https://doi.org/10.4203/cc.1.10.6>
- Hochuli A, Trouillet J.-G., Brühwiler E, Schulz O, Hoffmann M, "Renewal of a fixed railway track using UHPFRC – part 2", *Bautechnik*, 2022, *Volume 99*, pp 10-17, <https://doi.org/10.1002/bate.202100040>
- Shen X, Brühwiler E, "Influence of local fiber distribution on tensile behavior of strain hardening UHPFRC using NDT and DIC". *Cement and Concrete Research*, 2020, *Volume 132*, <https://doi.org/10.1016/j.cemconres.2020.106042>
- Shen X, Brühwiler E, Peng W "Biaxial flexural response of Strain-Hardening UHPFRC circular slab elements". *Construction and Building Materials*, 2020, *Volume 255*, <https://doi.org/10.1016/j.conbuildmat.2020.119344>
- Oesterlee C, Structural Response of Reinforced UHPFRC and RC Composite Members, doctoral thesis, Swiss Federal Institute of Technology Lausanne (EPFL), Lausanne, Thèse N°4848(2010).
- Makita T, Brühwiler E, "Damage models for UHPFRC and R-UHPFRC tensile fatigue behaviour, "Engineering Structures, Bd. 90, pp. 61-70, 2015, <https://doi.org/10.1016/j.engstruct.2015.01.049>
- Eligehausen R, A. Cook R, Appl J, "Behavior and Design of Adhesive Bonded Anchors, "ACI Structural Journal, vol. 103, Nr. 6, pp. 882-832, 2006, <https://doi.org/10.14359/18234>
- Satoh A, Sakagami Y, Mitarai S, "Finite Element Analysis on Pull-out Behavior of Post-installed Adhesive Anchor Filled with UHPFRC," Proceedings of the AFGC-ACI-fib-RILEM International Conference on Ultra-High Performance Fibre-Reinforced Concrete, Montpellier, France, 2017.
- Kalthoff M, Raupach M, "Pull - out behaviour of threaded anchors in fibre reinforced ordinary concrete and UHPC for machine tool constructions," *Journal of Building Engineering*, Vols. 33, no 2021, no. 2021, 2020, <https://doi.org/10.1016/j.jobe.2020.101842>
- Fehling E, Lorenz P, "characterisation of rebars anchorage in UHPC, "in RILEM-fib-AFGC Int. Symposium on Ultra-High Performance Fibre-Reinforced Concrete, Marseille, France, 2013.
- Grzesiak S., Pahn M., Schultz-Cornelius M., Susanne Bies N., "Influence of Different Fiber Dosages on the Behaviour of Façade Anchors in High-Performance Concrete," MDPI CivilEng, 2021, <https://doi.org/10.3390/civileng2030031>
- Červenka Consulting s.r.o., FEM Programm ATENA (Vers. 5.7.0), Praha, 2021.
- Červenka V, Jendele L, Červenka J, ATENA Program Documentation Part 1, Theory, Prague, 2021.
- De Borst R, "Non-linear analysis of frictional materials, "TU Delft, Delft, 1986, <http://resolver.tudelft.nl/uuid:d52ac7f8-d56f-4e0c-ab14-455ed02fcffe>.
- Cervenka J, Cervenka V, Laserna S, "On crack band model in finite element analysis of concrete fracture in engineering practice, "Engineering Fracture Mechanics, Bd. 197, pp. 27-47, 2018
- Pukl R, Novák D, Sajdlová T, Lehký D, Červenka J, Červenka V, "Probabilistic design of fibre concrete structures," in IOP Conference Series: Materials Science and Engineering, Prague, Czech Republic, 2017
- Hochuli, A., Brühwiler, E., "Numerical Simulation of the Structural Behavior of Threaded Anchors in UHPFRC", 3th International Interactive Symposium on Ultra-High Performance Concrete 2023, Wilmington, Delaware, USA, June 4-7, 2023

18. Hochuli, A., Brühwiler, E., "Failure Mechanism of Threaded Anchors in UHPFRC as Simulated by Finite Element Analysis", 4th International Symposium on Ultra-High Performance Fibre-Reinforced Concrete (UHPFRC), Menton, France, October 21-23, 2024

Disclaimer/Publisher's Note: The statements, opinions and data contained in all publications are solely those of the individual author(s) and contributor(s) and not of MDPI and/or the editor(s). MDPI and/or the editor(s) disclaim responsibility for any injury to people or property resulting from any ideas, methods, instructions or products referred to in the content.